RSC Advances

PAPER

View Article Online
View Journal | View Issue

Cite this: *RSC Adv.*, 2019, **9**, 31070

Activating molecular oxygen with Au/CeO_2 for the conversion of lignin model compounds and organosolv lignin†

Wu-Lin Song,[a] Qingmeng Dong,[a] Liang Hong,[ab] Zhou-Qi Tian,[a] Li-Na Tang,[a] Wenli Hao[a] and Hongxi Zhang *[a]

Received 26th June 2019
Accepted 25th September 2019

DOI: 10.1039/c9ra04838c

rsc.li/rsc-advances

Au/CeO_2 was demonstrated to be a high efficiency catalyst for the conversion of 2-phenoxyacetophenol (**PP-ol**) employing O_2 as an oxidant and methyl alcohol as the solvent without using an erosive strong base or acid. Mechanistic investigations, including emission quenching experiments, electron spin-resonance (ESR) and intermediate verification experiments, were carried out. The results verified that the superoxide anion activated by Au/CeO_2 from molecular oxygen plays a vital role in the oxidation of lignin model compounds, and the cleavage of both the β-O-4 and C_α–C_β linkages was involved. Au/CeO_2 also performed well in the oxidative conversion of organosolv lignin under mild conditions (453 K), producing vanillin (10.5 wt%), methyl vanillate (6.8 wt%), methylene syringate (3.4 wt%) and a ring-opened product. Based on the detailed characterization data and mechanistic results, Au/CeO_2 was confirmed to be a promising catalytic system.

Introduction

Despite their excellent performance and broad applicability, fossil fuel reserves are dwindling and their use causes environmental pollution. Green and renewable resources are considered key to the continuous development of society. Lignocellulosic biomass can continuously and steadily provide chemicals and fuel with zero net carbon emissions. In recent years, there has been increasing interest in the industrial production of organic compounds and fuels from lignocellulosic biomass.[1] As a primary constituent of lignocellulosic biomass (15–30% by weight and 40% by energy),[2] lignin consists mainly of three monolignols: coniferyl alcohol, sinapyl alcohol and *p*-coumaryl alcohol (seen Fig. 1). Based on its structure, lignin can be considered a source of value-added chemicals, such as aromatic aldehydes, ketones, acids and esters. The annual output of lignin in nature is 150 billion tons. More than 70 million tons of lignin are annually produced by the paper industry, and historically, most of this material is burned to provide energy.[3] As a nonedible and renewable biomass, lignin is a potentially valuable feedstock to produce organic compounds, especially high-value aromatics.[4,5] Efficiently depolymerizing lignin into well-defined aromatics represents a key challenge that limits the valorization of lignin.[6] In the past decade, increasing attention has been paid to the catalytic depolymerization of lignin in academia and industry.[7–9] Many efforts have focused on utilizing and manipulating the inherent structure and functionality of lignin,[10,11] especially the most abundant type, β-O-4 linkages, because they make up approximately 50% of all linkages, making them key to any depolymerization strategy.[4]

The best strategy for the depolymerization of lignin is still under debate. Traditional strategies have been based on catalytic cracking, hydrolysis, hydrogenolysis, reduction and oxidation.[12–16] Of these strategies, catalytic oxidization has received substantial attention due to its potential for yielding more highly functionalized monomers or oligomers, which are widely applicable in the chemical industry. Several attempts

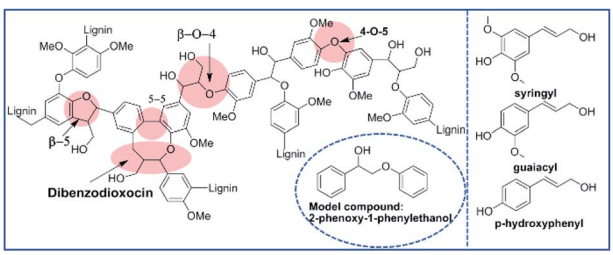

Fig. 1 The basic structural units and connections in lignin.

[a]*Department of Chemistry and Applied Chemistry, Changji University, Changji 831100, Xinjiang, China. E-mail: cjxyzhx@sina.cn*

[b]*Product Quality Inspection Institute of Changji Hui Autonomous Prefecture, Changji 831100, Xinjiang, China*

† Electronic supplementary information (ESI) available: TEM, XRD and XPS; lignin model compounds synthesis and cycling tests on Au/CeO_2. See DOI: 10.1039/c9ra04838c

have been made toward an economically practical catalytic oxidative decomposition of lignin to generate acids or aldehydes using O_2 as the oxidant with a heterogeneous catalyst.[17,18] In recent years, Au nanoparticles (NPs) supported on metal oxides (Au/MnO_2, Au/TiO_2, Au/CeO_2, *etc.*) have been investigated to selectively catalyze the aerobic oxidation of alcohols to the corresponding carbonyl compounds.[19–21] Very recently, Yang Song, *etc.* discussed a Au/hydroxide catalyst in which an alcohol was converted to the corresponding carbonyl by a two-electron process.[22] To date, however, there has been little discussion of the performance of Au/CeO_2 in the catalytic conversion of lignin.

In this paper, we introduce a heterogeneous catalyst, Au/CeO_2, for the depolymerization of lignin under molecular oxygen. The high catalytic activity of Au/CeO_2 with the lignin model compounds, the study of the reaction mechanism and the application of this catalyst to the conversion of lignin to aromatics are highlighted in this manuscript.

Experimental

Materials and methods

Preparation of CeO_2 nanorods.[23] First, 25.2 g of NaOH and 1.73 g of Ce $(NO_3)_3 \cdot 6H_2O$ were dissolved in 70 and 10 mL of deionized water, respectively, in beakers. These two suspensions were then mixed together in a Teflon bottle and stirred for 1 h at room temperature. Then, the Teflon bottle was placed in an autoclave and heated in an oven at 373 K for 72 h. The solid products were recovered by centrifugation, washed, and dried at 343 K for 12 h. Finally, the solid sample was calcined at 873 K in air for 6 h.

Preparation of Au/CeO_2.[24] First, 0.5 g of CeO_2 was added to 50 mL of an aqueous solution of 2.2×10^{-3} M $HAuCl_4$ with 0.22 M urea. The suspension was vigorously stirred for 4 h at 353 K and then centrifuged. The solid was washed with deionized water, dried at 343 K overnight and calcined at 573 K in air for 4 h, other metal oxides are treated in the same way.

Catalyst characterization

A 50 mg sample of the catalyst was transferred into a U-shaped quartz reactor and purged with He at 403 K for 3 h. Then, after cooling to ambient temperature, the flowing gas was switched to 5% H_2/Ar, and the sample was heated from room temperature to 973 K at a rate of 10 K min^{-1}. The X-ray diffraction (XRD) patterns of the catalyst were recorded using a Rigaku MiniFlex 600 diffractometer system. The morphology of the prepared Au/CeO_2 was observed by TEM on a Jeol 2100F electron microscope. X-ray photoelectron spectroscopy (XPS) measurements of the Au/CeO_2 were recorded on a Thermo SCIENTIFIC ESCALAB 250Xi. The binding energies were referenced to the C 1s level of adventitious carbon at 284.6 eV. The electron spin-resonance (ESR) signals were recorded on a Bruker EMX-10/12 spectrometer. The settings for the ESR spectrometer were as follows: center field, 3500.00 G; sweep width, 150.00 G; microwave frequency, 9.85 G; power, 3.99 mW; conversion time, 40.0 ms.

Catalytic test

All catalytic reactions were carried out in an 80 mL autoclave reactor. First, 0.47 mmol or 0.1 g of substrate, 20 mg of catalyst and 25 mL of methanol were added to a stainless steel autoclave. Then, the reactor was pressurized with 1 MPa O_2 and heated to the target temperature under mechanical stirring. The products were analyzed *via* HPLC and GC-MS (see the ESI†). The conversion and the selectivity of conversion of the substrate were calculated according to the following equations:

$$\text{Conversion} = \text{The mole of converted substrate/The mole of total substrate} \times 100\ (\%)$$

$$\text{Yield} = \text{The mole of the product/The total mole of the substrate} \times 100\ (\%)$$

Results and discussion

Characterizations of the materials

The phase purity and crystal structure of the catalyst were determined by XRD, and the results are displayed in Fig. S1.† Diffraction peaks from the (111), (200), (220), (311), (222), (400), (331) and (420) planes of CeO_2 are consistent with a cubic fluorite-type structure (JCPDS Card No. 65-2975). Obviously, the strong diffraction peaks confirm the high crystallinity of the sample. At the same time, no additional peaks were observed, which means that the prepared CeO_2 has better phase purity. After loading the Au NPs on the CeO_2 support, no Au peaks were observed in the spectrum of 0.88 wt% Au/CeO_2, suggesting an ultralow loading of Au, a particle size less than 5 nm, and a good dispersion of the Au NPs on the support. (The actual loading weight content was 0.88 wt%, as determined by ICP-AES analysis).

The transmission electron micrographs (Fig. S2†) show the presence of Au NPs with an average particle size of 5 nm on the as-prepared Au/CeO_2. The observed lattice spacing of 0.23 nm and 0.31 nm lattice fringes, which correspond to the Au (111) and CeO_2 (111) atomic planes, are in good agreement with the XRD results (Fig. S1†).[25]

The H_2-TPR data from the CeO_2 nanorods and Au/CeO_2 catalysts are shown in Fig. S3.† The pure CeO_2 nanorods do not exhibit a reduction peak at 293-773 K.[26] For the Au/CeO_2 catalyst, significant changes due to the reaction/absorption of hydrogen on the solid were observed. Four reduction peaks, at 398 K, 523 K, 661 K and 869 K, were present. The Au species in the Au/CeO_2 catalyst were reduced at 373–473 K. The peak at 398 K is attributed to Au reduction, while the peaks at 523 K and 661 K are attributed to the reduction of surface oxygen by CeO_2, and the reduction peak at 869 K is attributed to the lattice oxygen.[27] This indicates that the deposition of the Au NPs on ceria remarkably alters the catalytic activity and reducibility of the catalyst.

To further clarify the chemical states of the Au NPs, XPS analysis was conducted, as shown in Fig. S4.† The XPS spectrum of Au 4f displays typical doublet peaks with binding energies of

83.9 eV (Au $4f_{7/2}$) and 87.6 eV (Au $4f_{5/2}$), indicating that Au is present in its elementary metallic form.[28]

Metal oxides catalyze the oxidative of lignin model compound

The diffusion limit was eliminated by optimizing the agitation speed before the catalytic experiments (Fig. S5†). We found that when the rotation speed reached 400 rpm, the internal and external diffusion phenomena were controlled.

Based on this result, we tested the catalytic activities of several typical metal oxides and metal oxide-supported Au in the oxidative conversion of 2-phenoxy-1-phenylethanol (**PP-ol**). The results are shown in Table 1. When several of the typical metal oxides or no catalyst were used, the substrate displayed a very low conversion of 0.1–2.7% (Entries 1–5). When the Au NPs were loaded into metal oxides, the **PP-ol** was effectively converted to benzoic acid (**BA**), methyl benzoate (**MB**), **phenol**, dimethoxytoluene (**DT**), methyl phenylglyoxylate (**MP**) and uncleaved product 2-phenoxy-1- phenylethanone (**PP-one**) (Entries 6–9). Compared to several typical metal oxides (Entries 1–5), Au loaded on a metal oxide significantly accelerates the conversion of **PP-ol**. Au/CeO_2 showed the highest **PP-ol** conversion (71.5%). **Phenol**, **MB**, **PP-one** and **DT** were the major products with yields of 45.3%, 31.4%, 20.8% and 6%, respectively (Entry 9). The appearance of **MB** also demonstrates that the cleavage of the C_α–C_β bond is accompanied by the breakage of the β-O-4 linkage. Stahl *et al.* recently developed a novel methodology for the conversion of lignin into aromatic compounds under mild conditions.[9,29] This method involves the catalytic conversion of a C_α–hydroxyl group into the ketonic group and the subsequent cleavage of the β-O-4 bond. This strategy was developed by Deng and coworkers.[4] Because **PP-one** was also detected as a product (Table 1, Entry 6–9), we investigated its behavior under catalytic conditions. The results are shown in Table 2.

PP-one is transformed into the major products *i.e.*, **Phenol**, **BA** and **MB**, with a conversion of 21% (Table 2) without a catalyst. Compared with **PP-ol**, it reacted more quickly under the same operating conditions because **PP-one** also contains a β-O-4 bond, but the C_α–OH moiety is converted to a C_α=O group in **PP-ol**. This reactivity is consistent with the idea that the breakage of the β-O-4 linkage is easier when a C_α=O is present instead of a C_α–OH moiety.[29]

Then, we investigated the oxidative activity of Au/CeO_2 catalysts with different Au loadings (the actual loadings (weight content) were determined by ICP-AES analysis). As shown in Fig. 2, when the Au loading was increased from 0.08 wt% to 0.88 wt%, the conversion of **PP-ol** significantly increased from 25% to 71%. These results suggest that the Au NPs play a key role in the catalytic conversion of the substrate. Au NPs may enrich and activate molecular oxygen, greatly reducing the absorption energy of the reactants, as Wang reported.[30] Because Au NPs provide active sites for **PP-ol** oxidation in the Au/CeO_2 systems, increasing the number of Au active sites enhances the catalysis. However, it should be noted that the increase in the **PP-ol** conversion and the yield of **Phenol** and **MB** decreased as the Au loading exceeded 0.88 wt%. Moreover, the yield of **DT** increased significantly with increasing Au loading, and **DT** may be an intermediate in repolymerization, making it undesirable in the reaction system.

Both β-O-4 bonds and methoxy groups at various substitution positions are abundant in the aromatic units of lignin, and those methoxy groups may influence the activation of the β-O-4 linkages. Therefore, we investigated the oxidative performance of Au/CeO_2 for the catalytic transformation of substituted **PP-ol** at 453 K. As displayed in Table 3, the substituted compound is more reactive than **PP-ol**. When a CH_3O moiety was present, more than 90% the model compound was converted to the corresponding esters and phenols. This result indicates that Au/

Table 1 Catalytic conversion of PP-ol over several metal oxides[a]

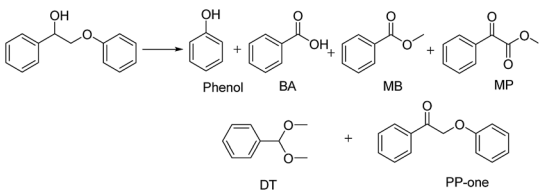

Entry	Cat.	Cons. (%)	Yield (%) Phenol	DT	BA	MB	PP-one	MP
1	Blank	<0.1	0	0	0	0	0	0
2	SiO_2	<0.1	0	0	0	0	0	0
3	Al_2O_3	2.9	0.5	0	0.24	2	0.9	0
4	Pr_6O_{11}	1.7	0.7	0	0.1	0	0	0
5	CeO_2	2.7	0	0	1.7	1.3	1.7	0
6	Au/SiO_2	54.8	9.5	1.9	21.2	24.6	18	0
7	Au/Al_2O_3	62.7	45.1	14.6	15.4	4.3	14.9	7.1
8	Au/Pr_6O_{11}	44.8	25.1	6.7	26.2	4.3	17.4	14.6
9	Au/CeO_2	71.5	45.3	6	4	31.4	20.8	6.7

[a] Reaction conditions: substrate, 0.1 g (0.47 mmol); catalyst, 20 mg; CH_3OH, 25 mL; O_2, 1 MPa; 453 K; 4 h.

Table 2 Catalytic conversion of PP-one over several metal oxides[a]

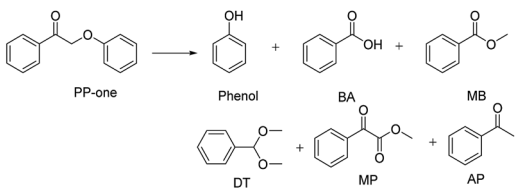

Entry	Catalysis	Cons. (%)	Yield (%) Phenol	DT	BA	MB	MP	AP
1	Blank	21	15	0	9.2	3.8	0	0
2	Al_2O_3	23	20	0	8.2	4.2	0	0
3	SiO_2	26	19	0	13	4.6	0	0
4	CeO_2	76	58	0	2.8	56	0	4.7
5	Au/CeO_2	>99	71.1	1.5	12.3	58.6	6.8	0

[a] Reaction conditions: **PP-one**, 0.1 g (0.47 mmol); catalyst, 20 mg; CH_3OH, 25 mL; O_2, 1 MPa; 443 K; 2 h.

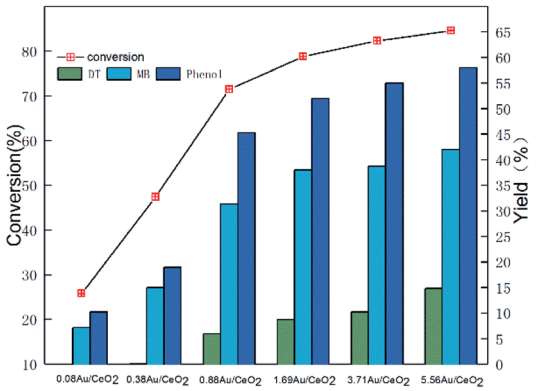

Fig. 2 Effect of Au loadings on the catalytic behaviors of Au/CeO_2 for the oxidation of **PP-ol**. Reaction conditions: **PP-ol**, 0.1 g (0.47 mmol); catalyst, 20 mg; CH_3OH, 25 mL; O_2, 1 MPa; 453 K; 4 h.

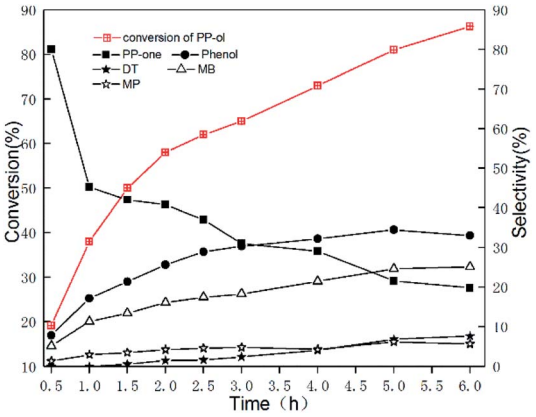

Fig. 3 Time course for the oxidation of **PP-ol** catalyzed by Au/CeO_2. Reaction conditions: 0.1 g (0.47 mmol); catalyst, 20 mg; CH_3OH, 25 mL; O_2, 1 MPa; 453 K.

Table 3 Catalytic performances of Au/CeO_2 for the conversion of substituted **PP-ol** model compounds[a]

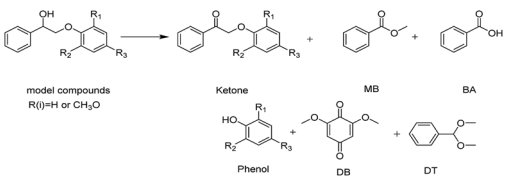

Substrate	Cons. (%)	Yield (%) MB	BA	Phenol	DB	DT	Ketone
	>99	82.5	1.7	85.3	0	1.9	6.4
	98.2	73.7	5.6	72	0	3.7	10.2
	94.7	60.7	4.3	1.7	70.2	6.7	15.4

[a] Reaction conditions: substrate, 0.47 mmol; Au/CeO_2, 20 mg; CH_3OH, 25 mL; O_2, 1 MPa; 453 K; 4 h.

CeO_2 performs well in the catalytic oxidative cleavage of β-O-4 in the lignin model compounds.

The stability of the Au/CeO_2 catalyst for the oxidative conversion of **PP-ol** was investigated (Fig. S7†). The catalyst could be recycled four times without a significant decline in its oxidative activity, and its product distribution remained stable. The reduction in the conversion may be attributed to an increase in the size of the Au NPs or a change in the catalyst surface properties, such as the presence of adsorbed products on the Au/CeO_2 or the oxidization of the catalyst surface.

Reaction mechanism for the oxidation of PP-ol

To elucidate the reaction pathway, we examined the oxidation of **PP-ol** over time on the Au/CeO_2 catalyst, and the results are shown in Fig. 3. As Fig. 3 shows, **PP-one** was the main product in the initial stage of the reaction with ~80% selectivity. As the oxidation progressed, the selectivity for **PP-one** rapidly decreased, and the selectivities for **Phenol**, **DT** and **MB** increased. After 4 h, the difference in selectivity became less significant. Subsequently, we calculated the concentration of the products, and depicted the changing trend of products concentration *vs.* time, as Fig. S6† shows. These findings support the hypothesis that the reaction proceeded through **PP-one** as an intermediate, and **PP-one** was further oxidized over the Au/CeO_2 catalyst. These results further indicate that the Au NPs play a key role in the oxidation of **PP-ol** by catalyzing the conversion of C_α-OH to $C_\alpha = =O$. A carbonyl compound was formed, and cleavage of the β-O-4 and $C_\alpha-C_\beta$ bonds subsequently occurred. Such a preoxidation process may reduce the energy barrier for the breakage of the β-O-4 linkage. Gregg T. Beckham *et al.* previously reported that by converting the C_α-hydroxyl group to a C_α-carbonyl, the β-O-4 bond dissociation enthalpy was reduced from 69.5 to 60.6 kcal mol^{-1}.[31]

To further investigate the role of O_2, we probed the effect of O_2 pressure in the catalytic system. We observed a 29% transformation of **PP-ol** with 0.1 MPa O_2 (Table 4, entry 1). **PP-one**,

Table 4 Catalytic conversion of **PP-ol** under different O_2 pressures[a]

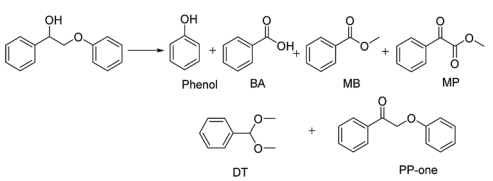

Catalysis	Cons. (%)	Yield (%) Phenol	DT	BA	MB	MP	PP-one
O_2 (0.1 Mpa)	29	15.1	4.90	5.1	5.5	0	8.3
O_2 (1 Mpa)	71.5	45.3	2	4	31.4	6.7	20.8
N_2 (1 Mpa)	0.7	0	0	0	0	0	0

[a] Reaction conditions: **PP-ol**, 0.1 g (0.47 mmol); catalyst, 20 mg; CH_3OH, 25 mL; 453 K; 4 h.

Phenol and **MB** were the major products. An increase in O_2 pressure efficiently promoted the conversion, suggesting that O_2 facilitates the breakage of both the C_α–C_β and β-O-4 bonds (Table 4, Entry 2).

When N_2 was employed, only a 0.7% conversion of **PP-ol** (Table 4, Entry 3) was observed. This finding suggests that Au/CeO_2 cannot catalyze this reaction in the presence of N_2, but the cleavage of the β-O-4 linkage could occur in the absence of O_2.

It was also confirmed that **PP-one** could more readily than **PP-ol** undergo this transformation because **PP-one** contains a β-O-4 bond adjacent to a C_α=O moiety, while **PP-ol** has a C_α–OH group. However, we observed 17% conversion of **PP-one** in the presence of N_2 (Table 5, Entry 3), which is obviously lower than the conversions (56%, >99%) under O_2 (Table 5, Entry 1 and 2). Interestingly, **phenol** and acetophenone were the major products, and they were obtained in yields of 15.2 and 14%, respectively. The appearance of **MB** confirms that the β-O-4 linkage was cleaved.

Radical trapping experiments

p-Benzoquinone is a scavenger of superoxide radicals,[32] and it was added to the reactor along with the substrate, and the results are presented in Table 6.

As displayed in Table 6, the conversion of **PP-ol** reached 71.5% (entry 1) in the absence of *p*-benzoquinone. However, when benzoquinone was added to the system, the conversion of **PP-ol** dropped dramatically (Entry 2–4) from 10.7% to 0.1% with increasing loading of the radical scavenger. When **PP-one** was used as the substrate, similar results were observed. These results demonstrated that a radical species played a vital role in the catalytic oxidation of the lignin model compounds; thus, we speculate that the oxidation occurred *via* a free radical process.

To verify this hypothesis, more mechanistic information was obtained by identifying the surface intermediates using *in situ* liquid-phase ESR spin-trapping experiments, as Fig. 4 shows. Data were acquired from a suspension of 0.1 g Au/CeO_2 sample in methanol with DMPO and oxygen. An obvious 6-fold signal characteristic of the superoxide radical anion was observed in the ESR data, suggesting that oxygen is activated by Au/CeO_2 to form superoxide anion free radicals.[28,33] Therefore, these experiments confirm that the Au/CeO_2 catalyst can strongly activate oxygen.

Employing molecular oxygen as the oxidant is green, economical, and attractive from an environmental viewpoint.[34] Efficiently catalyzing the reactions between inert, ground triplet-state O_2 ($^3\Sigma_gO_2$) and organic molecules (mainly in singlet-state) is key to this process. Substantial effort has been devoted to activating O_2 into active oxygen species.[35] Au NPs show a unique ability to generate superoxide radicals ($O_2^{\bullet-}$) through electron transfer processes.[36]

Tsukuda *et al.* reported that molecular oxygen is activated through negatively charged Au NPs to form a peroxo species or superoxide, which can then activate C–H bonds.[37] As Woodham *et al.*[38] demonstrated, electrons can be added to the O_2 π* orbital of O_2 *via* electron donation from loaded Au NPs, generating elongated O–O bonds that closely resemble those of the superoxo-like (O_2^-) adsorbate state. The oxidation process is subsequently accomplished through a series of deprotonation and elimination steps, *i.e.*, adsorbed molecular O_2 obtains an electron from Au/CeO_2 to generate Au/CeO_2–$O_2^{\bullet-}$, which then reacts with **PP-ol** to form **PP-one**. Based on the results presented and discussed above, a possible mechanism for the oxidation of **PP-ol** over the Au/CeO_2 catalyst is proposed in Scheme 1.

Table 6 Radical tripping experiments[a]

Entry	Substrate	Radical scavenger equivalent	Cons. (%)
1	**PP-ol**	—	71.5
2	**PP-ol**	0.1	10.7
3	**PP-ol**	0.5	7
4	**PP-ol**	1	<0.1
5[b]	**PP-one**	—	>99
6[b]	**PP-one**	0.1	42

[a] Reaction conditions: **PP-one**, 0.1 g (0.47 mmol); catalyst, 20 mg; CH_3OH, 25 mL; 453 K; O_2, 1 MPa; 2 h. [b] 443 K; 2 h.

Table 5 Catalytic conversion of **PP-one** under different O_2 pressures[a]

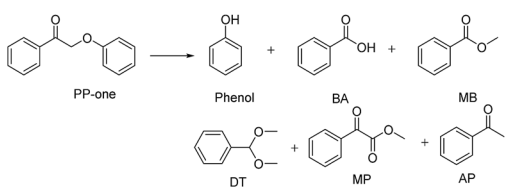

Catalysis	Cons. (%)	Yield (%)					
		Phenol	**DT**	**BA**	**MB**	**MP**	**AP**
O_2 (0.1 Mpa)	56	39	0.7	16.9	24	5	0
O_2 (1 Mpa)	>99	71.1	1.5	12.3	58.6	6.8	0
N_2 (1 Mpa)	17	15.2	0	0	0	0	14

[a] Reaction conditions: **PP-one**, 0.1 g (0.47 mmol); catalyst, 20 mg; CH_3OH, 25 mL; 443 K; 2 h.

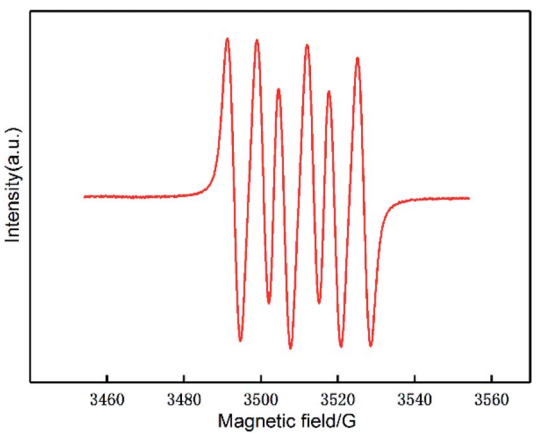

Fig. 4 ESR spectrum of DMPO-$O_2^{\bullet-}$ recorded in a system containing methanol, the catalyst and O_2 at 453 K.

To investigate the breakage of the β-O-4 linkage, the oxidation of several potential intermediates by Au/CeO_2 in an O_2 atmosphere at 453 K was explored (Fig. 5). First, phenylglyoxal can be fully converted to the corresponding breakage products, *i.e.*, **Phenol**, **DT**, **BA** and **MB** (eqn (1) in Fig. 5). These products are in good agreement with the products of the Au/CeO_2-catalyzed oxidation of **PP-ol** (Table 1). Because phenylglyoxal was also detected as a minor product by GC-MS, phenylglyoxal may be the intermediate in the oxidation, and it would presumably be produced from the breakage of β-O-4 linkage. Second, benzaldehyde showed a low conversion (10.2%) to **BA**, **MB** and **DT** (eqn (2)). Benzaldehyde is stable under the reaction conditions, suggesting that little of its C_α–C_β bond was broken. **BA** also showed a low transformation (24.4%) to **MB** (eqn (4)), indicating that **MB** was mainly formed from phenylglyoxal (eqn (1)). Third, methyl phenylglyoxylate showed a conversion of 32.9% under these conditions, and the major products were **MB**, **MA**, benzaldehyde and **DT** (eqn (3)). CO_2 was also released by this reaction (Fig. S8†). These results indicate that C_β is transformed *via* two pathways, including C_α–C_β bond and C_β–O bond breakage to CO_2 and methyl formate. Methyl phenylglyoxylate is stable in the reaction, meaning that it is not a possible intermediate.

Based on these results, a possible cleavage process for the oxidation was proposed (Scheme 2). In short, the C_α–hydroxyl group of **PP-ol** is primarily oxidized a C_α–carbonyl *via* the catalytic action of Au NPs. The subsequent oxidation of the β-O-4 linkage of **PP-one** over the Au/CeO_2 catalyst *via* $O_2^{\bullet-}$ could afford phenylglyoxal, methyl phenylglyoxylate and **phenol**. The catalytic breakage of the β-O-4 linkage over CeO_2 affords an oxidized intermediate (*e.g.*, phenylglyoxal) and **phenol**. A small amount of methyl phenylglyoxylate could also be produced in this process. The catalytically generated intermediate may undergo rapid oxidative cleavage of the C–C bond, generating **BA** and then **MB**, benzaldehyde and ultimately **DT**.

Our observations and mechanistic studies demonstrate the vital role of the preoxidation of the C_α–hydroxyl group. In our earlier research,[4] we loaded Au NPs onto commercial CeO_2 from Alfa Aesar. This material could also catalyze the transformation of **PP-ol** into monomeric aromatic compounds but a lower conversion than that achieved over Pd/CeO_2. However, when we changed the support to CeO_2 nanorods *via* a hydrothermal method and loaded Au NPs (<5 nm) on these rods, the prepared catalyst displayed excellent performance.

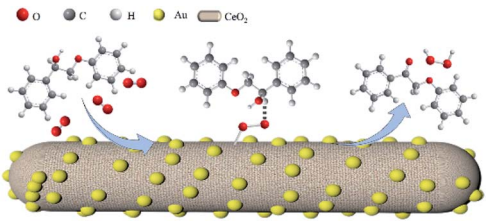

Scheme 1 Proposed mechanism for the aerobic oxidation of **PP-ol** over Au/CeO_2.

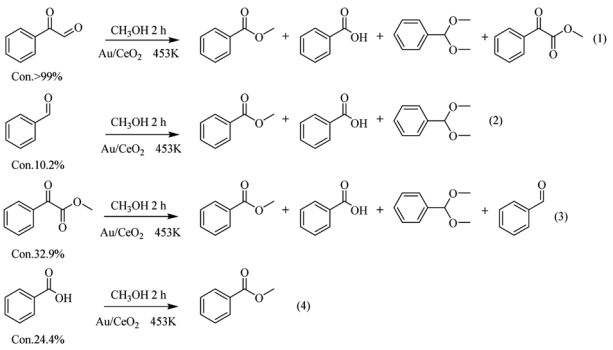

Fig. 5 Catalytic conversions of the possible intermediates under an O_2 atmosphere over Au/CeO_2.

Au/CeO_2-catalyzed conversion of real lignin

The oxidative conversion of organosolv lignin by the Au/CeO_2 catalyst system was subsequently investigated. Lignin was extracted *via* the ethyl alcohol-based organosolv process from cotton stalk according to a previous report. Then, the organosolv lignin was subjected to catalytic oxidation in methanol under O_2 with the Au/CeO_2 catalyst at 453 K for 4 h.

The results are displayed in Fig. 6. Several monomeric aromatic compounds, including vanillin (10.5 wt%), methyl vanillate (6.8 wt%), 2,6-dimethoxy-1,4-benzoquinone, methylene syringate (3.4 wt%) and a ring-opened compound, were detected and quantified by GC-MS. According to earlier reports, $LaMnO_3$ and $LaCoO_3$ are highly active for the catalytic oxidation of lignin to aromatic aldehydes, and they offer high yields of vanillin (~5%) and syringaldehyde (~10%).[39,40] Perovskite-type $LaFe_{0.8}Cu_{0.2}O_3$ materials have also been studied for the wet catalysis of lignin, and they provided maximum yields of vanillin and 4-hydroxylbenzaldehyde of 4.56 wt% and 2.49 wt%, respectively. However, an erosive strong base was required in these methods. Recently, a Pd/Al_2O_3 catalyst was reported for the oxidative conversion of alkaline lignin, affording only vanillin in a yield of 1.6 wt%.[41] Yang *et al.* investigated Au/Li–Al LDH materials, which showed excellent activity in the oxidation

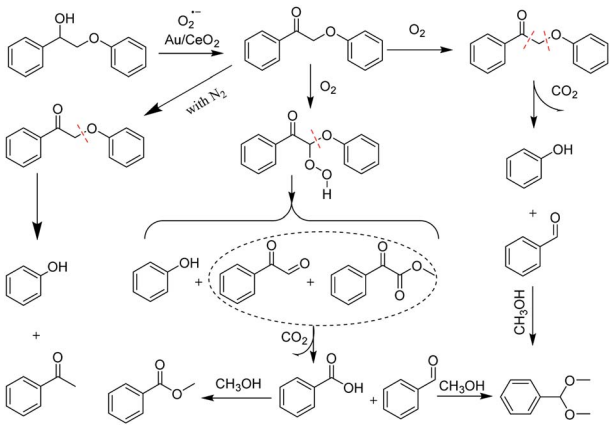

Scheme 2 Possible reaction mechanism for the oxidative conversion of **PP-ol**.

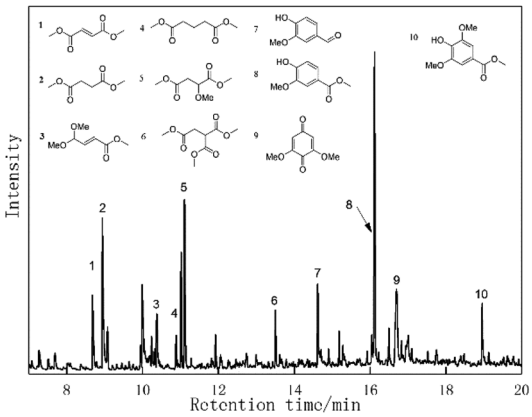

Fig. 6 GC-MS of products from Au/CeO_2-catalyzed organosolv lignin.

of natural lignin, and a 40 wt% yield of aromatic compounds was recorded from GVLox, while KLox afforded 10 wt% of desired compounds.[22] Our present results showed that Au/CeO_2 is also a promising material for the depolymerization of lignin to aromatic monomers in the absence of an erosive strong base or acid.

Conclusions

Au/CeO_2 was found to be a competent and environmentally friendly heterogeneous catalyst for the oxidation of model compounds and organosolv lignin using O_2 as the oxidant and methyl alcohol as the solvent. The ESR data suggests that a superoxide anion plays a vital role in the catalytic system. The highest conversion (95.3%) was obtained for the oxidation of 2-phenoxy-1-phenylethanol at 453 K with 1 MPa O_2 in 4 h. **Phenol**, methyl benzoate, 2-phenoxy-1-phenylethaone and dimethoxytoluene were the major products with yields of 45.3 wt%, 31.4 wt%, 20.8 wt% and 6 wt%, respectively. The Au/CeO_2 materials could also be employed for the direct oxidation of lignin, producing vanillin, methyl vanillate and methylene syringate in relatively high yields. Based on the above results, Au/CeO_2 is a promising catalyst system for the conversion of lignin to value-added low-molecular-weight aromatics.

Conflicts of interest

There are no conflicts to declare.

Acknowledgements

This work was supported by National Natural Science Foundation of China (21663002), and Education Department of Xinjiang Province (XJEDU2016I047).

Notes and references

1 J. Zakzeski, P. C. Bruijnincx, A. L. Jongerius and B. M. Weckhuysen, *Chem. Rev.*, 2010, **110**, 3552–3599.
2 C. Li, X. Zhao, A. Wang, G. W. Huber and T. Zhang, *Chem. Rev.*, 2015, **115**, 11559–11624.
3 Z. Sun, B. Fridrich, A. de Santi, S. Elangovan and K. Barta, *Chem. Rev.*, 2018, **118**, 614–678.
4 W. Deng, H. Zhang, X. Wu, R. Li, Q. Zhang and Y. Wang, *Green Chem.*, 2015, **17**, 5009–5018.
5 L. Shuai, M. T. Amiri, Y. M. Questell-Santiago, F. Héroguel, Y. Li, H. Kim, R. Meilan, C. Chapple, J. Ralph and J. S. Luterbacher, *Science*, 2016, **354**, 329–333.
6 P. Gallezot, *Chem. Soc. Rev.*, 2012, **41**, 1538–1558.
7 R. Gao, Y. Li, H. Kim, J. K. Mobley and J. Ralph, *ChemSusChem*, 2018, **11**, 2045–2050.
8 H. Guo, D. M. Miles-Barrett, A. R. Neal, T. Zhang, C. Li and N. J. Westwood, *Chem. Sci.*, 2018, **9**, 702–711.
9 A. Rahimi, A. Ulbrich, J. J. Coon and S. S. Stahl, *Nature*, 2014, **515**, 249.
10 Y. Liu, W. Chen, Q. Xia, B. Guo, Q. Wang, S. Liu, Y. Liu, J. Li and H. Yu, *ChemSusChem*, 2017, **10**, 1692–1700.
11 C. Xu, R. A. D. Arancon, J. Labidi and R. Luque, *Chem. Soc. Rev.*, 2014, **43**, 7485–7500.
12 T. Yoshikawa, T. Yagi, S. Shinohara, T. Fukunaga, Y. Nakasaka, T. Tago and T. Masuda, *Fuel Process. Technol.*, 2013, **108**, 69–75.
13 A. Das, A. Rahimi, A. Ulbrich, M. Alherech, A. H. Motagamwala, A. Bhalla, L. da Costa Sousa, V. Balan, J. A. Dumesic and E. L. Hegg, *ACS Sustainable Chem. Eng.*, 2018, **6**, 3367–3374.
14 M. Nagy, K. David, G. J. Britovsek and A. J. Ragauskas, *Holzforschung*, 2009, **63**, 513–520.
15 W. Schutyser, T. Renders, S. Van den Bosch, S.-F. Koelewijn, G. Beckham and B. F. Sels, *Chem. Soc. Rev.*, 2018, **47**, 852–908.
16 A. Bjelić, M. Grilc and B. Likozar, *Chem. Eng. J.*, 2018, **333**, 240–259.
17 S. G. Yao, J. K. Mobley, J. Ralph, M. Crocker, S. Parkin, J. P. Selegue and M. S. Meier, *ACS Sustainable Chem. Eng.*, 2018, **6**, 5990–5998.
18 B. Sedai, C. Díaz-Urrutia, R. T. Baker, R. Wu, L. P. Silks and S. K. Hanson, *ACS Catal.*, 2011, **1**, 794–804.
19 A. Abad, C. Almela, A. Corma and H. García, *Tetrahedron*, 2006, **62**, 6666–6672.
20 L.-C. Wang, Y.-M. Liu, M. Chen, Y. Cao, H.-Y. He and K.-N. Fan, *J. Phys. Chem. C*, 2008, **112**, 6981–6987.
21 L. M. Dias Ribeiro de Sousa Martins, S. A. C. Carabineiro, J. Wang, B. G. M. Rocha, F. J. Maldonado-Hódar and A. J. Latourrette de Oliveira Pombeiro, *ChemCatChem*, 2017, **9**, 1211–1221.
22 Y. Song, J. K. Mobley, A. H. Motagamwala, M. Isaacs, J. A. Dumesic, J. Ralph, A. F. Lee, K. Wilson and M. Crocker, *Chem. Sci.*, 2018, **9**, 8127–8133.
23 J. He, T. Xu, Z. Wang, Q. Zhang, W. Deng and Y. Wang, *Angew. Chem., Int. Ed.*, 2012, **51**, 2438–2442.
24 R. Zanella, L. Delannoy and C. Louis, *Appl. Catal., A*, 2005, **291**, 62–72.
25 Y. Liu, B. Liu, Q. Wang, Y. Liu, C. Li, W. Hu, P. Jing, W. Zhao and J. Zhang, *RSC Adv.*, 2014, **4**, 5975–5985.

26 M. F. Luo, Y. J. Zhong, X. X. Yuan and X. M. Zheng, *Appl. Catal., A*, 1997, **162**, 121–131.
27 X. Hong, Y. Sun, T. Zhu and Z. Liu, *Catal. Sci. Technol.*, 2016, **6**, 3606–3615.
28 Z. Cui, W. Wang, C. Zhao, C. Chen, M. Han, G. Wang, Y. Zhang, H. Zhang and H. Zhao, *ACS Appl. Mater. Interfaces*, 2018, **10**, 31394–31403.
29 A. Rahimi, A. Azarpira, H. Kim, J. Ralph and S. S. Stahl, *J. Am. Chem. Soc.*, 2013, **135**, 6415–6418.
30 Z. Wang, J. Qi, K. Zhao, L. Zong, Z. Tang, L. Wang and R. Yu, *Mater. Chem. Front.*, 2017, **1**, 1629–1634.
31 S. Kim, S. C. Chmely, M. R. Nimlos, Y. J. Bomble, T. D. Foust, R. S. Paton and G. T. Beckham, *J. Phys. Chem. Lett.*, 2011, **2**, 2846–2852.
32 S. M. Bonesi, I. Manet, M. Freccero, M. Fagnoni and A. Albini, *Chem. - Eur. J.*, 2006, **12**, 4844–4857.
33 Y. Ren, Y. Che, W. Ma, X. Zhang, T. Shen and J. Zhao, *New J. Chem.*, 2004, **28**, 1464–1469.
34 M. Liu and C. J. Li, *Angew. Chem., Int. Ed.*, 2016, **55**, 10806–10810.
35 H. Su, K.-X. Zhang, B. Zhang, H.-H. Wang, Q.-Y. Yu, X.-H. Li, M. Antonietti and J.-S. Chen, *J. Am. Chem. Soc.*, 2017, **139**, 811–818.
36 A. Roldán, J. M. Ricart, F. Illas and G. Pacchioni, *J. Phys. Chem. C*, 2010, **114**, 16973–16978.
37 S. Yamazoe, K. Koyasu and T. Tsukuda, *Acc. Chem. Res.*, 2013, **47**, 816–824.
38 A. P. Woodham, G. Meijer and A. Fielicke, *Angew. Chem., Int. Ed.*, 2012, **51**, 4444–4447.
39 H. Deng, L. Lin, Y. Sun, C. Pang, J. Zhuang, P. Ouyang, J. Li and S. Liu, *Energy Fuels*, 2008, **23**, 19–24.
40 H. Deng, L. Lin, Y. Sun, C. Pang, J. Zhuang, P. Ouyang, Z. Li and S. Liu, *Catal. Lett.*, 2008, **126**, 106.
41 J. Zhang, H. Deng and L. Lin, *Molecules*, 2009, **14**, 2747–2757.